CHAPTER IV

RESULTS AND DISCUSSIONS

4.1 Optimum Temperature for Calcination of Photocatalyst

After preparation of the dry gel of Ti/PVP through sol gel technique and drying by oven, determination of the temperature for crystalline formation was performed on TG-DTA. This temperature was used as the guideline for heat treatment (calcination). Calcination was employed to remove PVP and crystalline growth of TiO_2. The product after calcination was called as nanocrystalline TiO_2, which then was characterized by XRD, BET, SEM, and photocatalytic testing with phenol solution. Optimum temperature was indicated by the highest efficiency to degrade phenol solution, which was used in the determination of the optimum ratio of Ti:Sn.

4.1.1 Determination on-set temperature for nanocrystalline formation by Thermogravimetric-differential thermal analysis (TG-DTA)

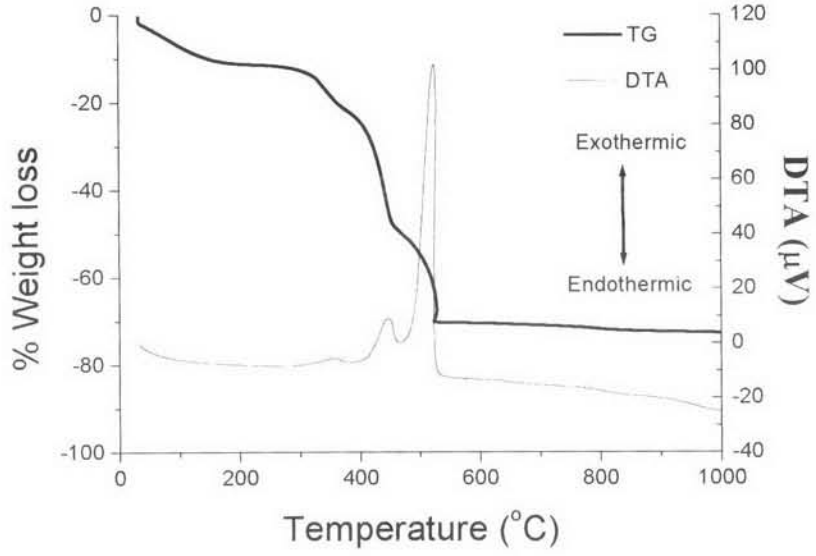

Figure 4-1 TG-DTA curves of thermal decomposition of dried gel Ti/PVP.

Figure 4.1 shows TG and DTA curves of the prepared Ti/PVP precursor. The total weight loss from TG curve was about 70 wt%. The TG curve shows a

small changing weight loss over 520°C. There were two main exothermic peaks in the DTA curve. The first exothermic broad peak at about 440°C indicated the loss of PVP from the precursor. The sharp peak at about 520°C presented the formation of anatase (Music et al. (1997), Yu et al. (2000)). It could be stated that nanocrystalline was initiated at 520°C. These temperatures in the range of 500-900°C were used in the calcination experiments.

4.1.2 Determination of TiO_2 photocatalyst Characteristics by XRD

Chataracteristics of both nanocrystalline TiO_2 synthesized at various temperatures from 500-900 °C (called as nanocrystalline TiO_2) and commercial TiO_2 were analyzed by XRD. The XRD patterns of nanocrystalline TiO_2 became sharper as the calcination temperature increased, implying that the nanocrystalline TiO_2 was turned into more ordered crystalline (Jung et al., 2005). At the calcination temperature of 500 °C, the predominant phase was anatase (JCPDS File No. 21-1272) as shown in Figure 4-2(a). The phase transition, anatase-to-rutile, gradually occurred at 600°C and most likely completed to the rutile (JCPDS File No. 21-1276) at 900 °C. The crystal sizes of synthesized TiO_2 nanoparticles at various temperatures are presented in Table 4-1. The crystallite sizes of the nanocrystalline TiO_2 both anatase and rutile phases were increased as increasing temperature. These results were the same trend as the previous studies (Music et al. (1997), Zheng et al. (2001), Li et al. (2002), Bessekhouad et al. (2003), Su et al. (2004) and Jung et al. (2005)). The size of the anatase crystallites was increased from 15 to 80 nm, whereas the commercial TiO_2 had crystallite size of 41 nm. Additionally, at the temperature below 800°C the anatase phase of the nanocrystalline TiO_2 had crystallite size of 39 nm which was close to the commercial product. Notably, the temperature between 700 °C and 800°C the crystallinity of nanocrystalline TiO_2 was not much changed. It was consistency with size of ~39 nm, and above this temperature the particle size was dramatically increased. The rutile phase revealed a different result. The crystallinity was increased from 101 nm to 201 nm. The particle sizes of the rutile phase were fairly increased as increasing temperature, and were greater than those of anatase phase at all temperatures.

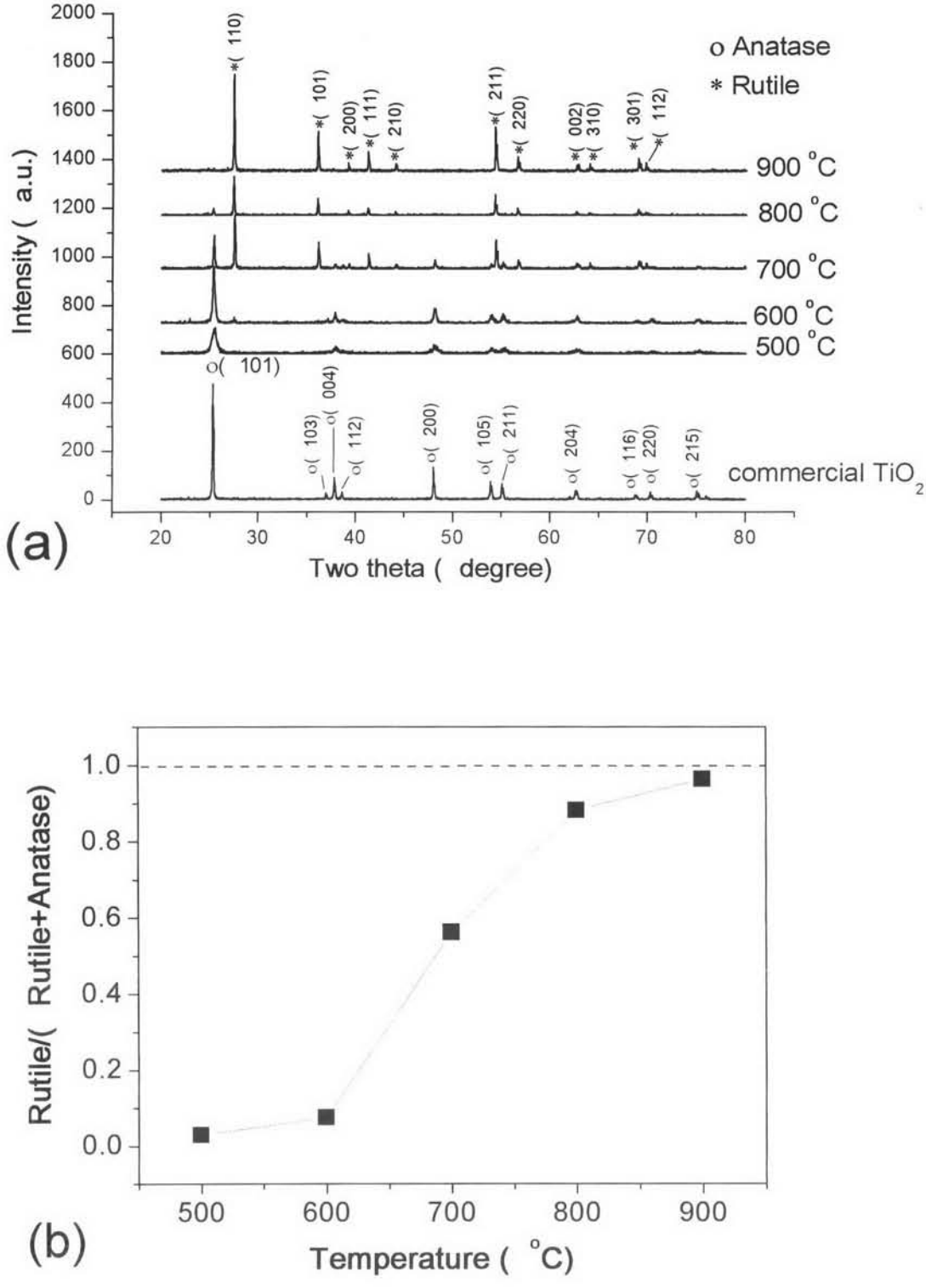

Figure 4-2 (a) XRD patterns of the synthesized TiO_2 nanoparticles at different temperatures. (b) Rutile content versus the sum of the anatase and rutile.

Table 4-1 Crystallite size of anatase/rutile phase and surface area (BET) at various calcination temperatures.

Calcined temperature	Crystallite size (nm)		Surface area
(°C)	Anatase (101)	Rutile (110)	(m^2/g)
500	15	-	31.8
600	29	101	12.9
700	39	114	4.1
800	39	190	3.2
900	80	201	2.6
Commercial TiO_2	41	-	10.8

As shown in Figure 4-2(b), the transformation of anatase-to-rutile was gradually increased at the temperature between 500 °C. and 600 °C. At the temperature exceeding 600 °C, the fraction of rutile was significantly increased with rising temperature. The explanation of such results was that the heat treatment at the higher temperature promoted the meta stable to stable of the phase transformation of anatase-to-rutile which could be defined as irreversible transformation (Kumar, 1995). Anatase phase was rather preferred than rutile phase for photocatalytic degradation. The phase characteristics relevant to temperature would play important role on photocatalytic performance that is going to further discussion.

4.1.3 Specific Surface Area

The results of surface area (BET) are presented in Table 4-1. Surface area of all samples was influentially changed by the thermal treatment temperature. The highest surface area of 31.8 m^2/g was found for the sample calcined at 500 °C. For the calcination temperatures from 600 °C to 900°C, the values of surface area drastically decreased from 12.9 to 2.6 m^2/g. The higher temperature would induce a larger crystal size, leading to decrease surface area. However, for the effective nanocrystalline material, the surface area and the fraction of rutile and anatase have to be co-performed. The temperatures from 500 to 900 °C were further used for photocatalytic activity.

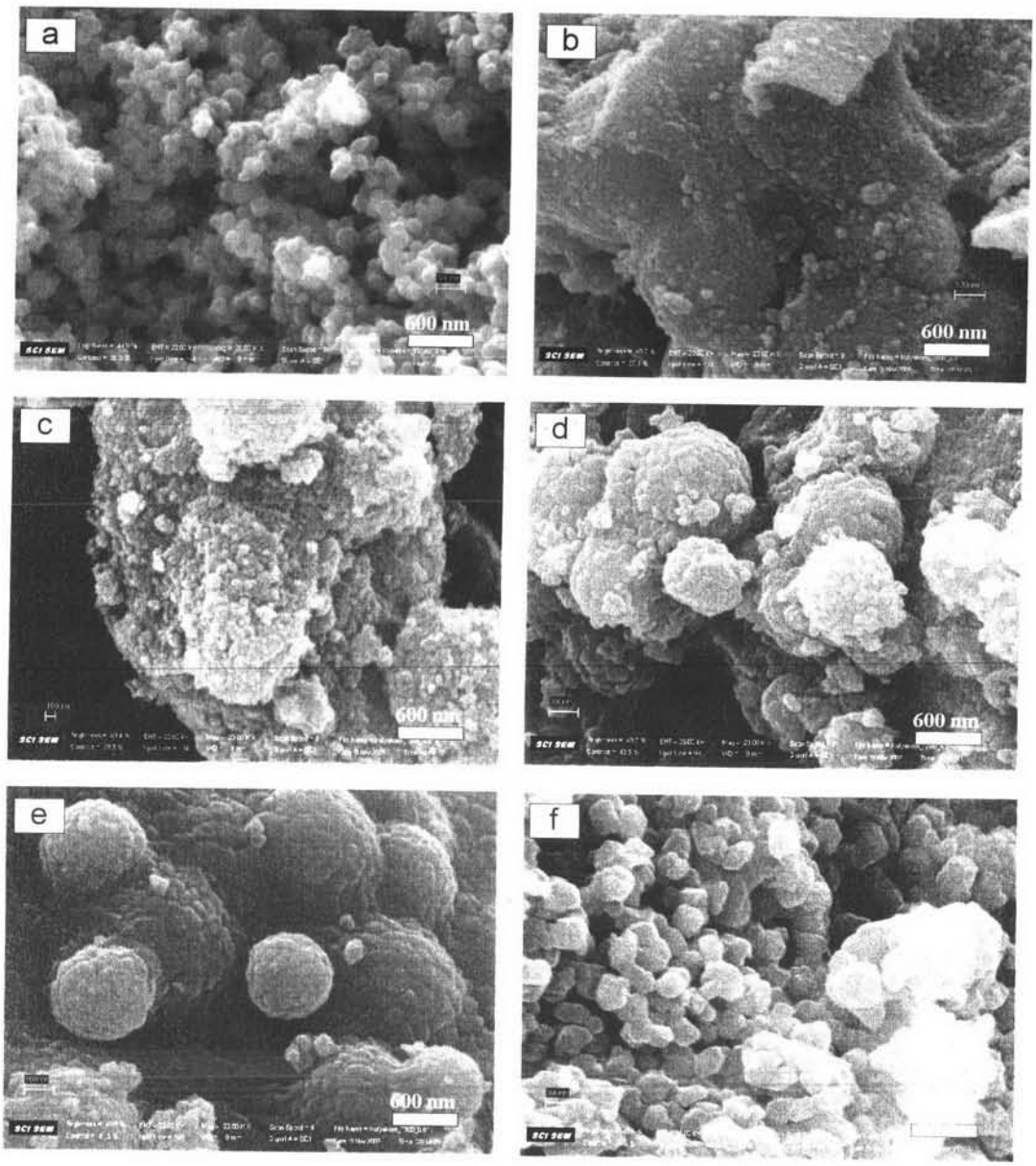

Figure 4-3 SEM images of commercial TiO_2 (a) and nanocrystalline TiO_2 calcined in air for 3 h at 500°C (b), 600°C (c), 700°C (d), 800°C (e), and 900°C (f). (Magnification: X 20 000).

4.1.4 Morphology of Photocatalysts by Scanning Electron Microscopy (SEM)

Morphologies of the nanocrystalline TiO_2 and commercial TiO_2 were revealed by SEM as shown in Figure 4-3. The commercial TiO_2 contained spherical particles with size of ~50 nm (Figure 4-3(a)), whereas the nanocrystalline TiO_2 samples consisted of agglomerated particles with sizes in the range of 20-200 nm. Agglomerates were evidently observed in the SEM micrographs for the samples calcined at high temperatures. Particle size increased with the increasing calcination temperature. The SEM results were confirmed by the results calculated from XRD line broadening. Morphologies which was observed from SEM image also reveled the increasing the rutile phase due to the increasing temperature as well.

4.1.5 Photocatalytic Testing

The results of photocatalytic testing are presented in Figure 4-4. This shows the relative concentration of phenol, C/Co, at the different time of UV irradiation. The concentrations at the various times are represented by C. The initial phenol concentration, Co, is the concentration after dark adsorption for 1 hour. The photocatalytic activity of the commercial TiO_2 sample was better than those of the nanocrystalline TiO_2 samples. It is noted that all the nanocrystalline TiO_2 samples had higher degree of agglomeration compared to the commercial TiO_2 sample. Therefore, the highest efficiency through the photocatalytic testing observed in the commercial TiO_2 sample was possible due to its low agglomeration and also well dispersion during suspension in the phenol solution. Among the nanocrystalline TiO_2 samples, the photocatalytic performance of the sample calcined at 600 °C yielded the fastest degradation. The results also revealed the decrease of photocatalytic efficiency with increasing the calcination temperature with the exception of the sample calcined at 600°C. In general, the anatase phase of TiO_2 has been recognized to perform the higher activity of photocatalysis than the rutile phase (Watanabe et al., 1999; Sumita et al., 2002). However, there is a report (Hurum et al., 2006) indicated that the mixed phase performing more efficiency than the pure anatase as those mixtures reduced the

recombination of electron and hole, leading to the increasing efficiency of photacatalysis. In this study, the highest efficiency for the nanocrystalline TiO_2 samples was obtained in the sample calcined at 600°C at which had the mixed phase of anatase (92.5%) and rutile (7.5%). It is possible that the mixed phase of anatase and rutile would reduce the recombination of electron and hole, which leaded to the increasing efficiency of photacatalysis in the 600°C-calcined sample.

It is worth noting that, although the 600°C-calcined TiO_2 samples showed slower degradation than the commercial TiO_2 sample. At the same level of degradation i.e. at C/Co of ~ 40%, it exhibited smaller amount intermediates than those of the commercial TiO_2 sample when observed with chromatogram of HPLC (Figure 4-5). Many reports on phenol oxidation (Janez and Albin, 1995; Santos et al., 2004; Suzuki et al., 2006) reveal an increase in toxicity near the beginning stages of degradation. The small amount of intermediate produced from degradation of phenol observed on the 600°C-calcined TiO_2 sample also indicated that the 600°C-calcined TiO_2 sample had less toxicity than the commercial TiO_2 sample.

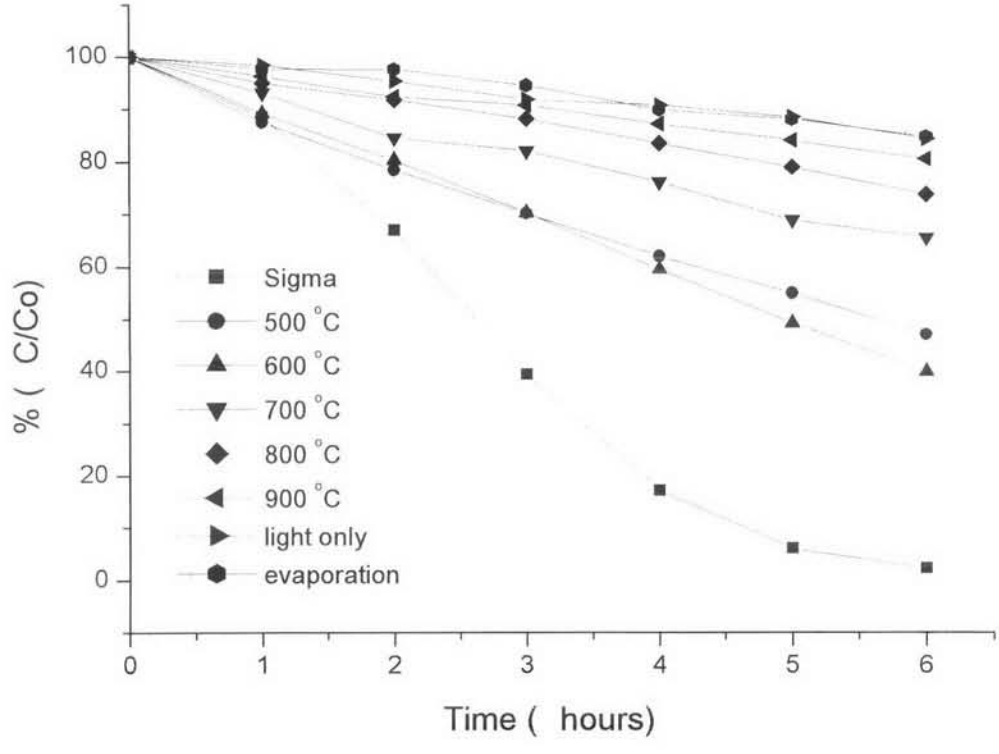

Figure 4-4 Relative concentration of phenol versus irradiation time.

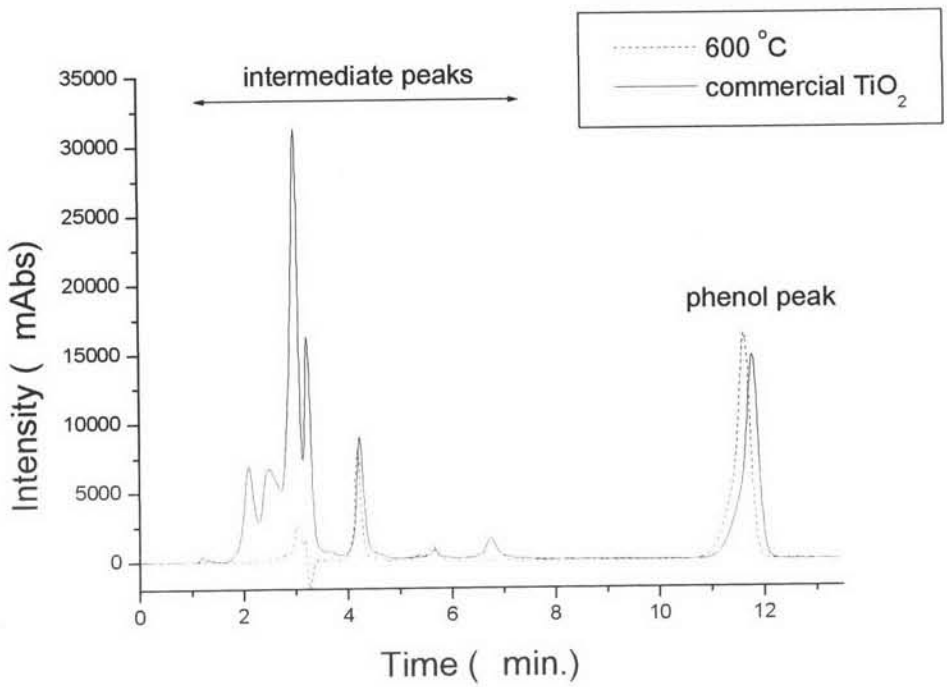

Figure 4-5 Intermediates of 600 °C and commercial TiO_2 at the degree of 60 percent degradation.

4.1.6 Summary

Nanocrystalline TiO_2 with particle sizes of 15-80 nm for anatase phase and 100-200 nm for rutile phase had been successfully synthesized by a simple modified sol-gel method using TIAA and PVP as starting materials. The prepared samples were characterized by TG-DTA, XRD, BET specific surface area and SEM. The highest surface area of 31.8 m^2/g was obtained for the TiO_2 sample calcined at 500 °C for 3 hours. However, the optimum calcination temperature for the nanocrystalline TiO_2 to achieve the highest photocatalytic degradation of phenol was 600 °C as influenced by the fraction of anatase to rutile of 92.5:7.5. Despite degradation efficiency of the nanocrstalline TiO_2 was lower than commercial TiO_2, the sample calcined at 600°C presented a smaller amount of intermediates throughout the phenol degradation than that of the commercial TiO_2.

4.2 Optimum Ratio of Titanium and Tin for Nano-photocatyst

To increase the photocatalytic efficiency by reducing the charge recombination, doping titanium dioxide with other metal oxide is one of alternative techniques. This section presents the determination of optimum ratio of titanium and tin (Ti:Sn) in the process of TiO_2 synthesis. The previous section mentions the optimum calcinations temperature was 600 °C. However from the previous reports mentioned the dopant (a little added substance) would increase the transformation of anatase-to-rutile. To investigate the optimum ratio of Ti:Sn, the cacination temperature was extended the range to the minimum temperature that could remove PVP, thus the calcinations temperature of 550 and 600 °C were carried out in this determination.

4.2.1 Determination of photocatalyst characteristics of Sn-doped TiO_2 by XRD

XRD pattern in Figure 4-6 shows a confirmation to the previous studies (Shannon and Pask, 1965: Richards, 2002) that the doping would increase the anatase-to-rutile transformation. Obviously, with addition of Sn in Ti/PVP, calcination temperature of 550 and 600 °C had different results on phase transformation. At 600 °C, XRD patterns exhibited a gradually smaller and broadening of sharp peak anatase (101) with increasing the mixing ratio of Sn. Meanwhile rutile (110) exhibited a higher sharper peak with increasing Sn. On the contrary, the temperature of calcination at 550 °C did not show a significant anatase-to-rutile transformation, it illustrated the broadening of peak anatase (101), implying that the crystalline size was smaller as an increasing of Sn.

A decrease crystalline size was confirmed by the calculation according to Scherer's equation. Calculation of crystalline size is shown in Table 4-2. As increasing ratio of Sn crystalline size, both of anatase and rutile slightly presented a smaller crystalline size. The smallest crystalline size of anatase, 11.75 nm, was existed by 3% of Sn by mole of Ti at calcination temperature of 550 °C. At this stage, temperature of 550 °C was seemed to perform better than 600 °C. However, both temperatures were tested for photocatalytic activities.

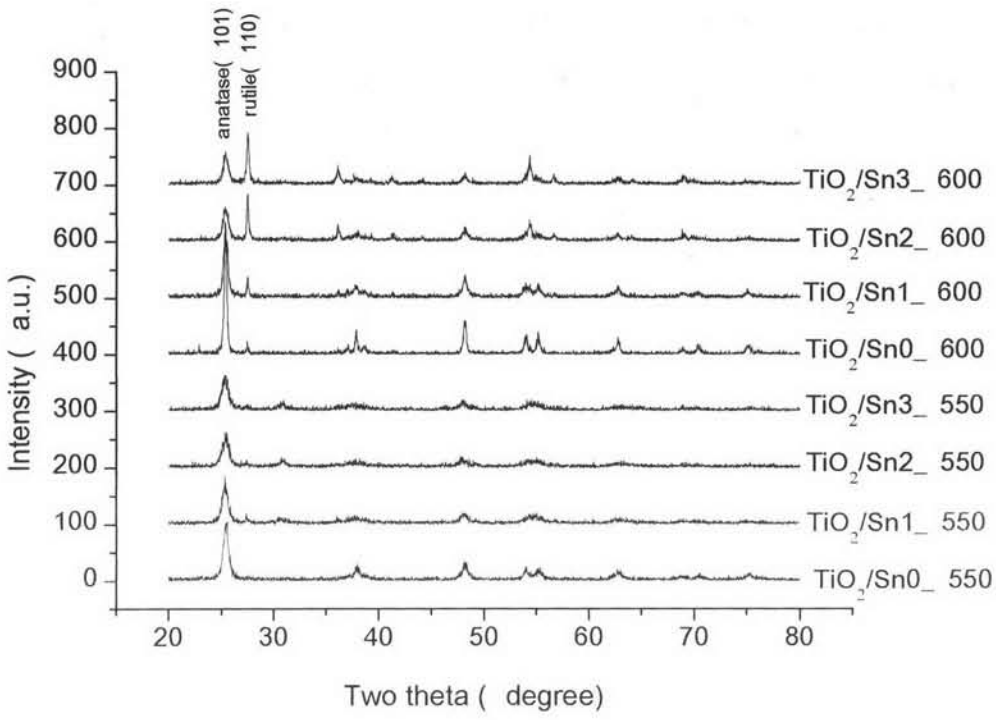

Figure 4-6 XRD patterns of calcined-TiO_2 with various ratio of Sn at calcination temperatures 550 and 600 °C.

Table 4-2 Properties of synthesized materials with various ratio of Sn at calcination temperatures 550 and 600 °C.

% Sn by mole of Ti	Temperature of calcination					
	550 °C			600 °C		
	Anatase (101)	Rutile (110)	Surface area (m^2/g)	Anatase (101)	Rutile (110)	Surface area (m^2/g)
0	19	-	24.2	29	101	12.9
1	13	106	56.7	20	160	31.8
2	13	47	65.6	13	116	53.2
3	11	67	90.2	15	91	55.7

4.2.2 Specific Surface Area

The results of surface area (BET) were presented in Table 4-2. Surface area of all samples was relatively changed by the mixing ratio of Sn. The highest surface area of 90.2 m^2/g was found for the sample calcined at 550°C with 3% Sn

of Ti. Noticeably, at the heat treatment of 600 °C without addition of Sn, the surface area was 12.93 m^2/g while increasing Sn by 1-3% of Ti the surface areas were increased from 31.80 to 55.74 m^2/g. At the calcined temperature of 550 °C, surfaces area was in the range of 24.2-90.2 m^2/g as increasing the Sn ratio. This indicated that Sn inhibited crystal growth, and promoted an increasing surface area. An increasing surface area would induce higher photocatalytic performance.

4.2.3 Morphology of compososite photocatalyst by SEM

Morphologies of the TiO_2 doping with Sn for all samples indicated less agglomeration than TiO_2 samples without Sn doping. Figure 4-7 shows the SEM image of TiO_2 with 2% Sn by mole of Ti at 550 °C heat treatment (TiO_2/Sn2). This image revealed a less agglomeration and uniform particles.

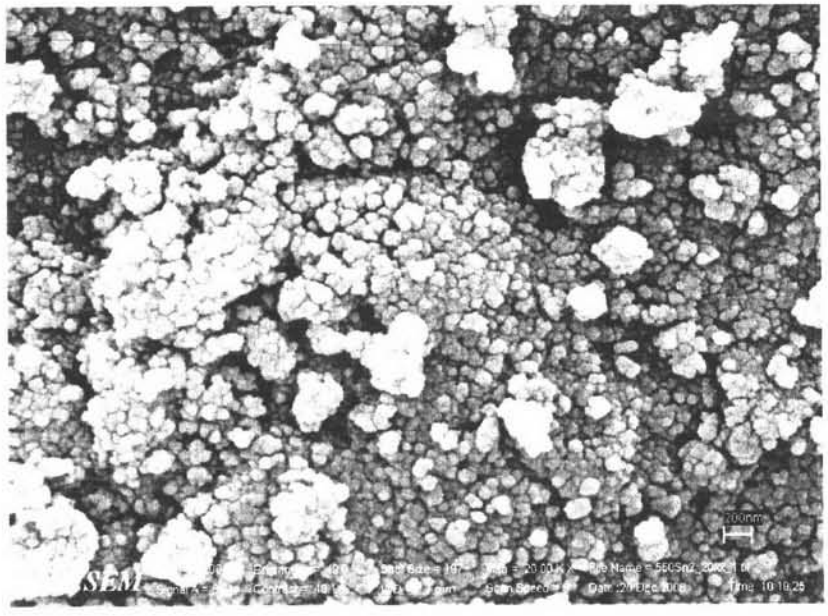

Figure 4.7 SEM image of TiO_2/Sn2 at 550 °C (Magnification: X 20 000).

4.2.4 Photocatalytic testing with Sn-doped TiO_2 photocatalyst

After 6 hours irradiation of phenol solution, the % remaining phenol solution versus %Sn by mole of Ti is illustrated in Figure 4-8. At the conditions of 550 and 600 °C, % remaining of phenol were similar in the range of 40-45% for

any mixing of % Sn. Except the lowest % remaining (32%) was existed by the mixing of 2% Sn. This occurrence was due to the fraction ratio of anatase and rutile. Based on calculation, the ratio of anatase to rutile was 92:8 for the 2% Sn at 550°C. This ratio was similar to the ratio was obtained from the nanocrystalline TiO_2 calcined at 600°C. It indicated that the sample with dopant of Sn 2% at lower temperature (550°C) performed a higher effective photocatalysis. The ratio of anatase and rutile plays important role on photocatlytic degradation of phenolic compound.

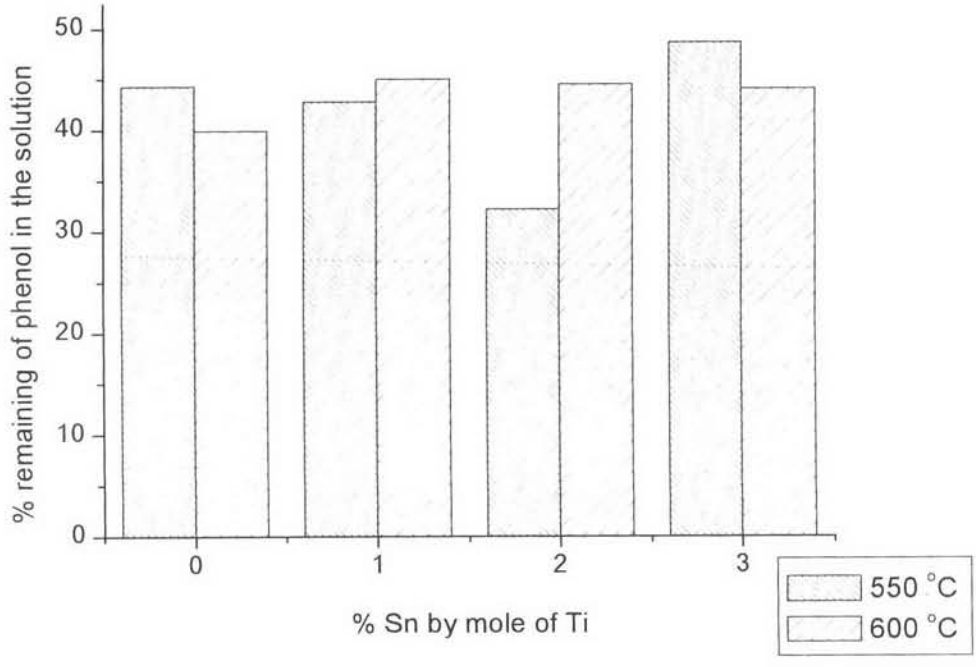

Figure 4-8 Percentage of remaining after 6 hours irradiation of phenol solution by synthesized TiO_2 at calcined temperature 500 and 600 °C.

4.2.5 Summary

This section reveals the effect of dopant to phase transformation of anatase-to-rutile and surface area of the synthesized nanocomposite. Addition of Sn promoted higher surface area, but in the mean time it accelerated transformation of anatase-to-rutile. The optimum temperature of calcination was changed from 600 to 550 °C for the case of doping with Sn. It is noted that at 600

°C while increasing the surface area, the rutile phase was also increased. Therefore, the efficiency of phenol degradation was not high. It was due to the influence of rutile phase rather than surface area. At 550 °C heat treatment, the percentage of doping Sn treatment did not show the effect any transforming of anatase-to-rutile, but only made the increment of surface area. Notably, 2 % mixing of Sn by mole of Ti and heat treatment at 550 °C yielded the fraction of anatase-to-rutile of 92:8. Again, the results indicated the role of anatase fraction on phenol degradation. However, the increased surface area would enhance photocatalytic degradation under the optimum ratio of anatase to rutile. This optimum ratio of anatase to rutile was conformed with the ratio of anatase to rutile as 92.5:7.5 showing the high efficiency of phenolic compound photocatalytic degradation at the calcination temperature at 600 °C.

In conclusion, the optimum conditions to synthesized TiO_2 were 2 % mixing of Sn by mole of Ti and heat treatment at 550 °C for 3 hours. The synthesized TiO_2 under the optimum conditions from now on was named as TiO_2/Sn2. This TiO_2/Sn2 was further used in the study of intermediates, photocatalytic testing of synthetic solution, and real wastewater.

4.3 The Occurrence of Photocatalytic Reaction's Intermediates

Intermediate is defined as the chemical species produced during the degradation of the primary compound. This section presents the chemical species produced during the photocatalytic degradation of phenolic compounds in the batch reactor. In reference with the preliminary study, the studied phenolic compounds included phenol, guaiacol, and syringal. Thus, the individual high concentration of phenol, guaiacol and syringol was irradiated for 6 hours with TiO_2/Sn2 and commercial TiO_2. The extracted sample was injected to GC/MS and the spectra were characterized by the library in computer software and some compounds were defined by comparing the retention time with the authentic compounds.

4.3.1 Intermediates from photocatalysis of phenol

As mentioned in the earlier section (Section 4.1 and Figure 4-5), by comparing the HPLC chromatogram, it demonstrated a smaller intermediate of

photocatalysis with TiO_2/Sn2 than the commercial TiO_2. The same results were also illustrated by GC/MS technique. The main intermediates of commercial TiO_2 were catechol and hydroquinone while only hydroquinone was detected from TiO_2/Sn2 (Table 4-3) (Figure 4-9).

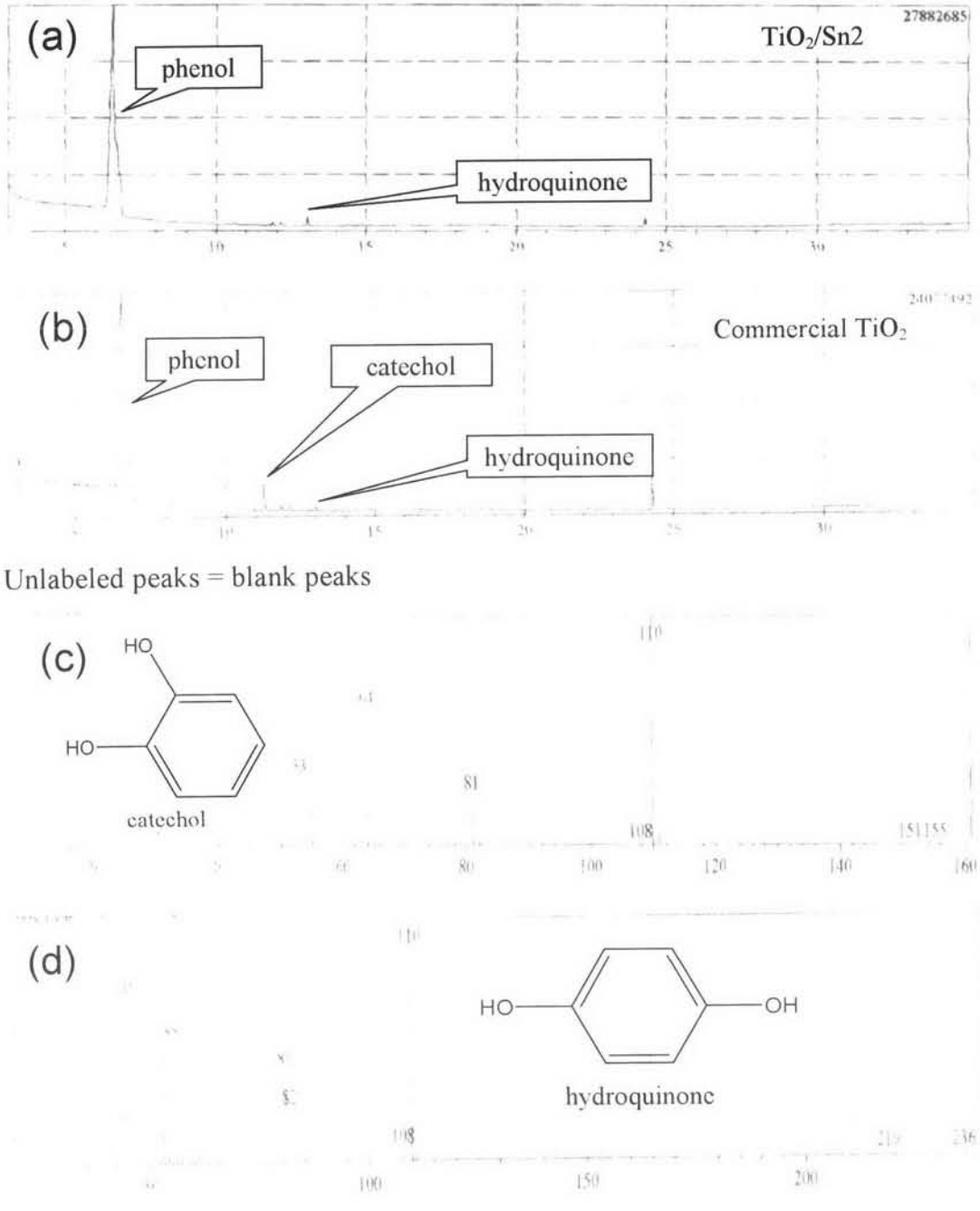

Figure 4-9 GC/MS Chromatogram of phenol solution after 6 hours irradiation with (a) TiO_2/Sn2 (b) commercial TiO_2 and mass spectrum of the detected intermediates (c) catechol and (d) hydroquinone.

Table 4-3 Intermediates from photocatalysis of phenol by photocatalysts TiO_2/Sn2 and commercial TiO_2.

Photocatalysts	Detected intermediates	Retention time (min.)	Identification technique
TiO_2/Sn2	Hydroquinone	13.03	Library and authentic compound
Commercial TiO_2	Catechol Hydroquinone	11.29 13.03	Library and authentic compound

The commercial TiO_2 illustrated the intermediates similar to the previous studies of Ohta et al. (1980), Devlin and Harris (1984), Duprez et al. (1996), Alejandre et al. (1998), Santos et al. (2002), and Nagaveni et al. (2004). These reports revealed catechol and hydroquinone as the intermediates by using a catalyst in the oxidation reaction of phenol. Astonishingly, the TiO_2/Sn2 presented only hydroquinone as its intermediate. This result was in conformance with the chromatogram interpreted from the HPLC.

4.3.2 Intermediates from photocatalysis of guaiacol

From Table 4-4, intermediate study of guaiacol oxidation by both catalysts, 1,2-Benzenediol and 2 –Methoxyresorcinal were the main intermediates for the commercial TiO_2. On the other hand, TiO_2/Sn2 did not show any intermediates which were able to detect by GC/MS technique under the condition setup in this study. This might be assumed that a type of column, detection limit of instrument, as well as a sample preparation were not compatible for doing the intermediate qualitative analysis of guaiacol (Figure 4-10).

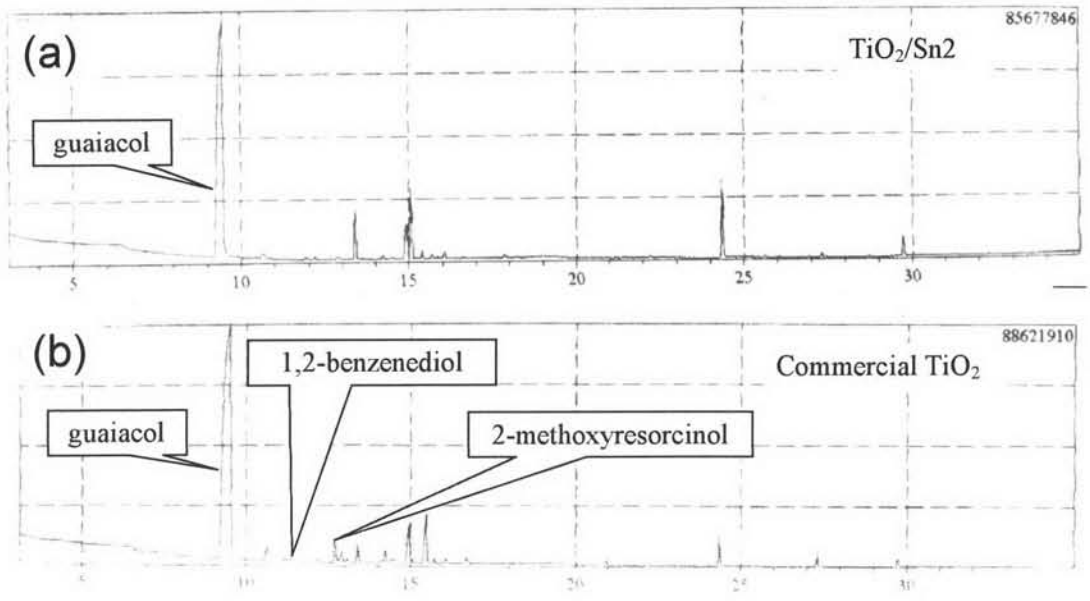

Unlabeled peaks = blank peaks, unidentified peaks

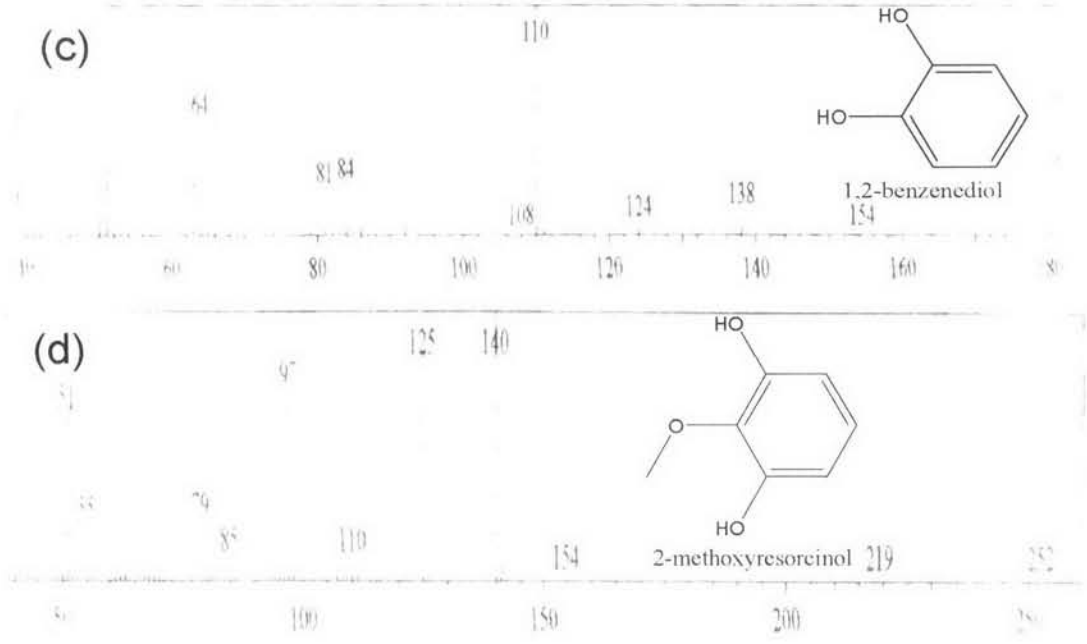

Figure 4-10 GC/MS Chromatogram of guaiacol solution after 6 hours irradiation with (a) TiO_2/Sn2 (b) commercial TiO_2 and mass spectrum of the detected intermediates (c) 1,2-benzenediol and (d) 2-methoxyresorcinol.

Table 4-4 Intermediates from photocatalysis of guaiacol by photocatalysts TiO_2/Sn2 and commercial TiO_2.

Photocatalyst	Detected intermediates	Retention time (min.)	Identification technique
TiO_2/Sn2	-	-	Library
commercial TiO_2	1,2-Benzenediol 2-Methoxyresorcinal	11.16 12.69	Library

4.3.3 Intermediates from Photocatalysis of Syringol

The syringol photocatalyst oxidation by TiO_2/Sn2 also presented a fewer of intermediates than the commercial TiO_2. The main intermediates of both catalysts were methylsyringol and allyl ester crotonic acid. Exception of 2-methoxyresorcinal was found to be intermediate for the commercial TiO_2 (Table 4-5) (Figure 4-11).

Table 4-5 Intermediates from photocatalysis of syringol by photocatalysts TiO_2/Sn2 and commercial TiO_2.

Photocatalyst	Detected intermediates	Retention time (min.)	Identification technique
TiO_2/Sn2	Methylsyringol Allyl ester crotonic acid	13.59 22.06	Library
Commercial TiO_2	2-Methoxyresorcinal Methylsyringol Allyl ester crotonic acid	12.70 13.56 22.08	Library

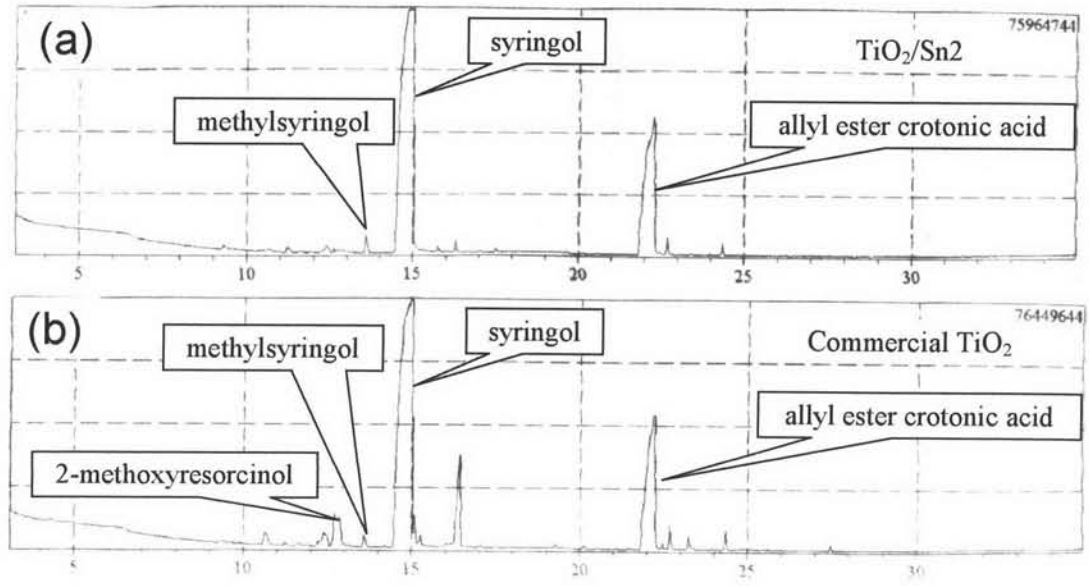

Unlabeled peaks = blank peaks, unidentified peaks

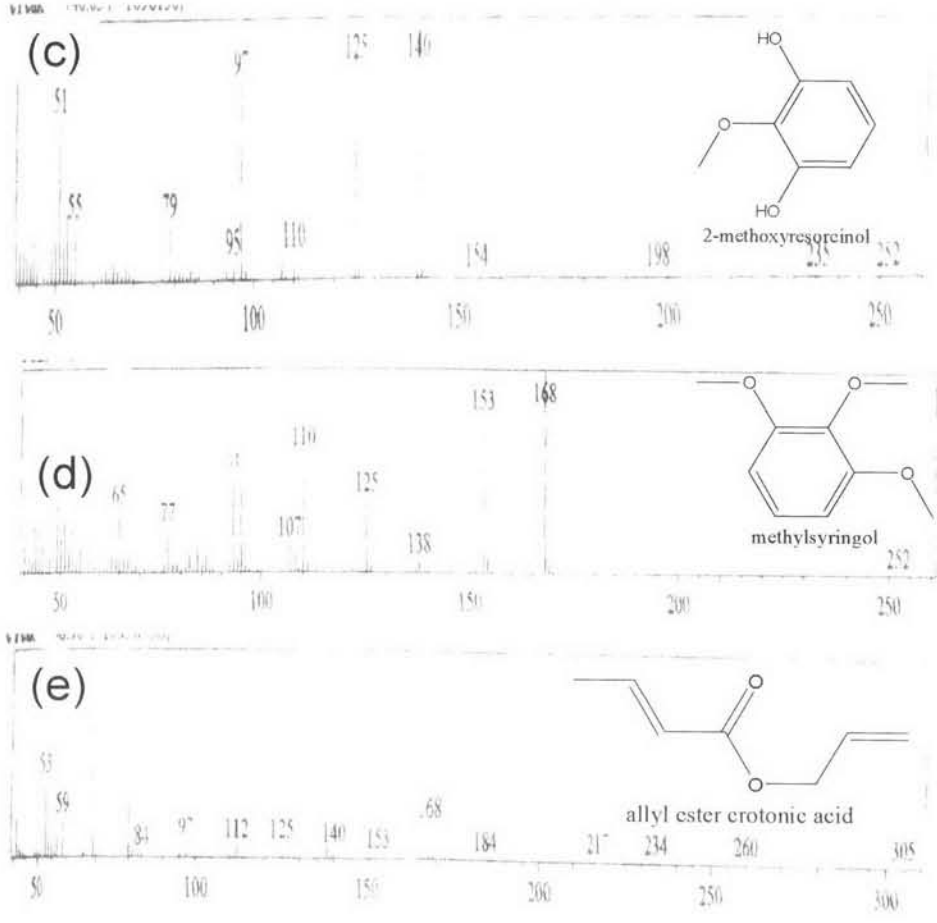

Figure 4-11 GC/MS Chromatogram of syringol solution after 6 hours irradiation with (a) TiO_2/Sn2 (b) commercial TiO_2 and mass spectrum of the detected intermediates (c) 2-methoxyresorcinol (d) methylsyringol and (e) allyl ester crotonic acid.

4.3.4 Summary

Regarding the intermediates produced during photocatalytic degradation of those three phenolic compounds, numbers of the intermediates produced by TiO_2/Sn2 and the commercial TiO_2 were different. All of photocatalysis of the studied phenolic compounds (phenol, guaiacol, and syringol) presented none to two intermediates produced when using TiO_2/Sn2. While two to three intermediates were produced when using the commercial TiO_2. As stated by Kohl et al (2005), the surface reactions of phenolic substances on tin oxide a dehydrogenation step is expected as illustrated in Figure 4-12. Therefore, the free hydroxyl groups are less than the one without tin. Accordingly, the reaction taken place at the hydroxyl group would be less, leading to less number of intermediates. It is noted that both the synthesized and commercial ones produced hydroquinone which is considered as harmful to environment. However, after completing degradation of the main phenolic compound, all intermediates would be substantially disappeared as indicated by Figure 4-13.

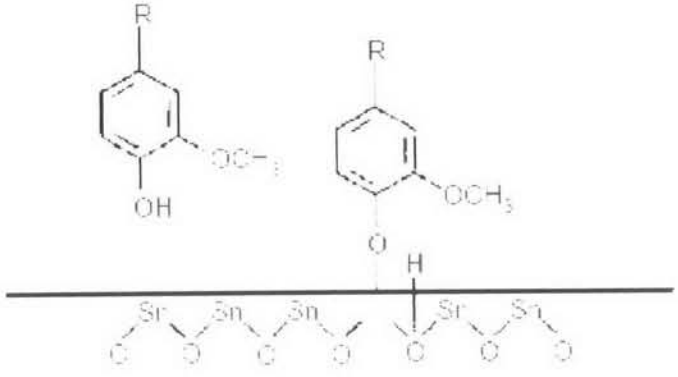

Figure 4-12 Surface Reaction of Phenolic Componds on Tin Oxide (Kohl et al., 2005)

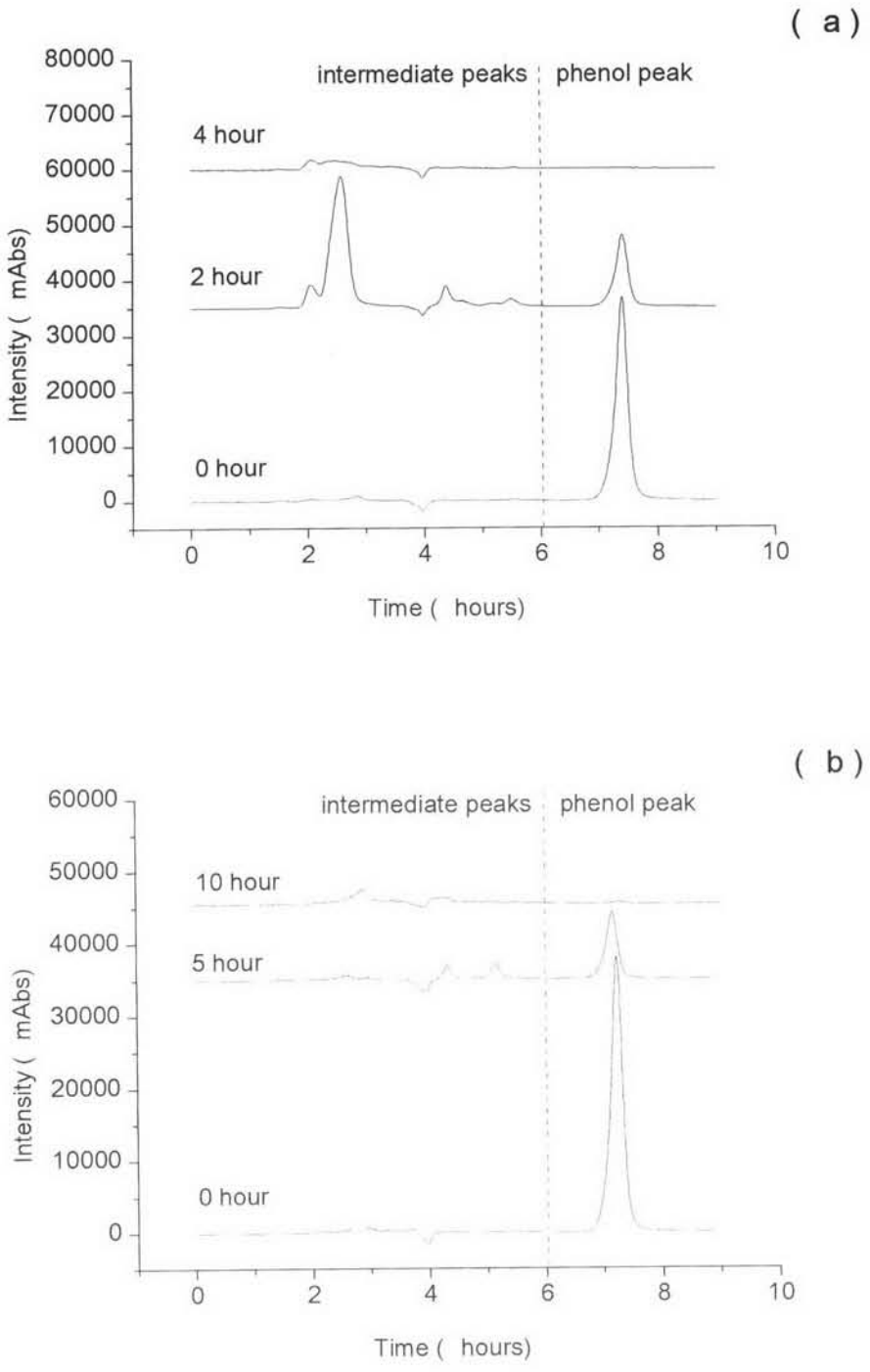

Figure 4-13 Disappearance of intermediates after complete photodegradation of phenol solution with (a) commercial TiO_2 (b) TiO_2/Sn2.

4.4 Photocatalytic Degradation of Phenolic Compounds

The experimental investigations were performed for the synthetic wastewater both individual and mixed solution of guaiacol, syringol, and phenol. Photocatalytic degradation is shown by the percentage remaining of phenolic compounds (C/Co, %) with irradiated time. Figures 4-14 (a) and (b) present the photocatalytic degradation with the synthesized TiO_2/Sn2 and commercial TiO_2 for the individual guaiacol, syringol, and phenol, respectively. For degradation with the synthesized TiO_2/Sn2, the sequence of higher degradation were syringol>guaiacol>phenol. Surface reaction was described for dehydrogenation of phenolic compound on tin oxide (Khol et al., 2005). Hydroxyl group are electron-donating substituents on a phenyl ring which are correlated with a high ability to be oxidized since methoxy phenols (guaiacol and syringol) have more electron-donating substituents than phenol. Thus, more surface reaction on tin oxide of methoxy phenols (guaiacol and syringol) than phenol as a result photooxidation efficiency showed the order as syringol>guaiacol>phenol. Outstandingly, the highest decomposition of syringol was performed after two hours of irradiation. After six hours irradiation, guaiacol and phenol were still remained as 1% and 32% respectively while the commercial TiO_2 presented the degradation in the reverse order with TiO_2/Sn2. The commercial TiO_2 showed the sequence of higher degradation as phenol>guaiacol>syringol. Phenol and guaiacol were almost decomposed but the syringol was still remained about 13% after six hours irradiation. For the individual phenol solution, electron-rich of double bond carbon-carbon, was easier oxidized by electrophilic addition reaction (Oppenlander, 2003). On the other hand, methoxy phenols (guaiacol and syringol) also have double bond of carbon-carbon but the methoxy ($-OCH_3$) group on their structure inhibiting the electrophilic addition reaction so they presented a less oxidized reaction by electrophilic addition reaction since the efficiency of degradation illustrated the order as phenol>guaiacol>syringol for the photodegradation of individual solution by commercial TiO_2.

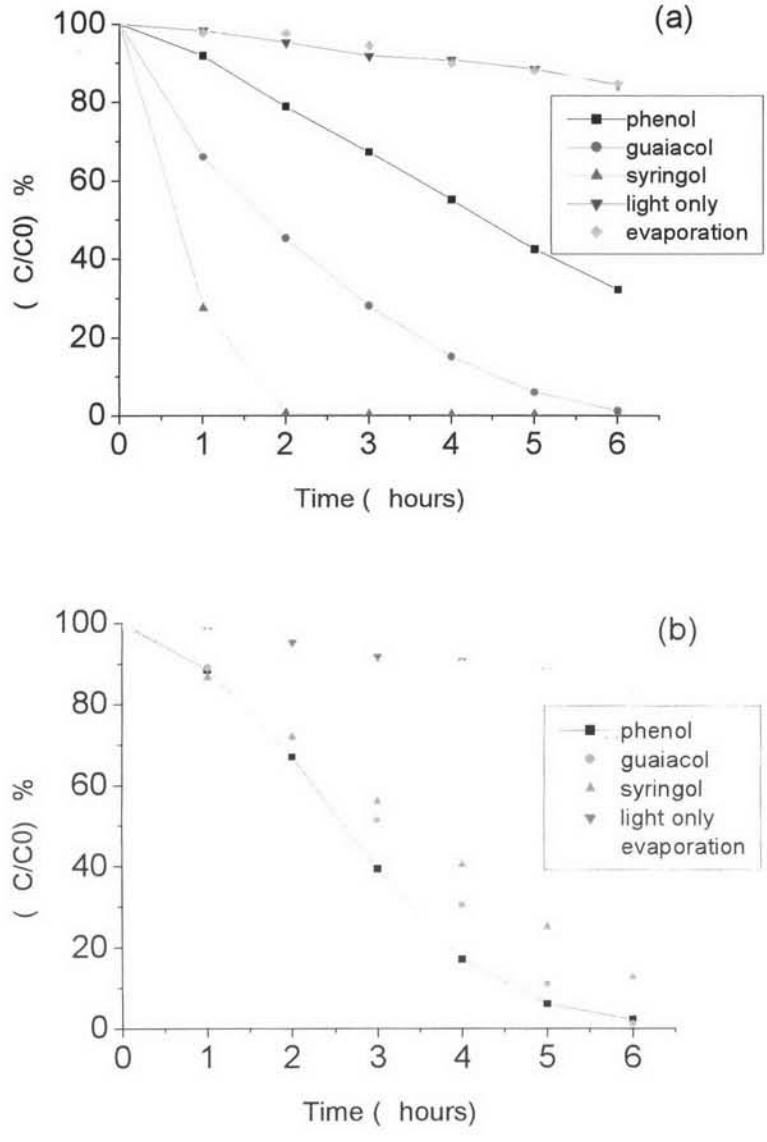

Figure 4-14 Relative concentration of phenolic compounds during its irradiation with (a) TiO_2/Sn2 (b) Commercial TiO_2.

The degradations of mixed phenolic compounds by TiO_2/Sn2 and commercial TiO_2 are shown in Figures 4-15 (a) and (b), respectively. TiO_2/Sn2 completely degraded syringol within three hours of irradiation. After six hours degradation, guaiacol and phenol were remained of about 9% and 75% respectively. Notably, the commercial TiO_2 resulted in a slower degradation for these three mixed compounds. The amount of remaining of syringol, guaiacol, and phenol were

about 26%, 37%, and 62% respectively. In addition, with the observation by chromatogram of HPLC, the degradation of phenolic compounds by the commercial TiO_2 showed the higher amount of the intermediates than TiO_2/Sn2. The intermediates during degradation of syringol and/or guaiacol probably effected to the degradation of phenol. These intermediates significantly affected to the mixed compounds degradation by the commercial TiO_2. In accordance with the characteristics of the catalysts, the combination of anatase and rutile phases of the synthesized TiO_2/Sn2 and only the anatase phase of the commercial TiO_2 would generate different intermediates. As described above, the intermediates generated by the synthesized one were less than the commercial one. Therefore, the inhibition of degradation of phenol in the mixed solution was accordingly lower. This inhibition of intermediates could also be seen by the degradation of individual solution of phenol compound and the mixed phenolic compound solution with the commercial TiO_2 which have only anatase phase, the degradation of phenol compound of the individual solution was significantly higher than the mixed one, and the sequence of degradation was reversed as stated above. While TiO_2/Sn2 presented the same order of degradation both of individual compound and mixed compounds solution. Moreover, as noted that phenol degradation in the mixed solution by both commercial and synthesized ones were much lower than syringol and guaiacol. The irradiation time might be one of the factors to be considered. As the irradiation time was set for 6 hours, the complete degradation might not be attained. It might need longer time than 6 hours for phenol degradation. Based on the observation on intermediates study for the individual solution of phenol (see Figure 4-13), it revealed that after irradiation about 10 hours phenol and intermediates had been disappeared. Again, for the mixed solution the degradation of phenol might be different due to the interference of intermediates as described above.

Another assumption to describe the photodegradation efficiency of mixed solution, the ability to be antioxidant of each compound are investigate by Radical scavenging power (RSP) (Brand-Williams et al., 1995) (see Appendix). RSP is the ability to be antioxidant, anti the free radical. RSP of phenolic compounds is shown in table 4-6. Phenol showed the lowest RSP while guaiacol and syringol showed the higher RSP respectively which means guaiacol and syringol trended to react with free radical (hydroxyl radical) in mixed solution rather than phenol

which has the lowest RSP. Since for both of commercial TiO_2 and TiO_2/Sn2 in mixed solution showed the order of efficiency of photodegradation as phenol<guaiacol<syringol.

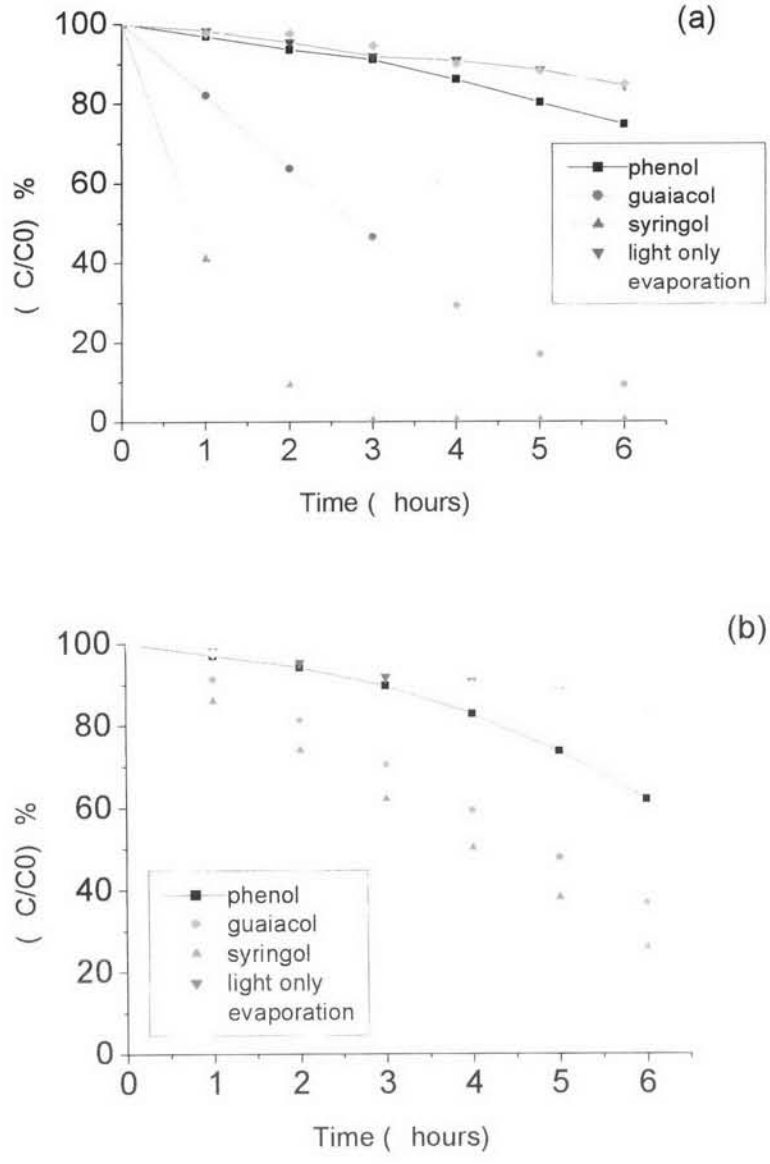

Figure 4-15 Relative concentration of mixed phenolic compounds during its irradiation with (a) TiO_2/Sn2 (b) Commercial TiO_2 .

Table 4-6 Radical scavenging power (RSP) of phenolic compound by DPPH method.

Phenolic compounds	RSP
Phenol	19.2
Guaiacol	35.3
Syringol	63.2

To support the previous discussion, the reaction rate of phenolics compounds is also discussed. The reaction rate of phenolic compounds degradation was determined with pseudo first-order reaction kinetics:

$$-\ln \frac{C}{Co} = k_{obs} t \qquad \text{.....(4-1)}$$

where:

Co is the initial concentration of phenolic compound

C is the concentration at the various time of phenolic compound (mg/L)

k_{obs} is the observed first-order rate constant(h^{-1})

t is time (h).

Table 4-7, all phenolic compounds degradation followed pseudo first-order reaction kinetics, which had R^2 values between 0.9109 and 0.9792. It was found that the degradation rates are accordance to the previous discussion. Syringol showed the highest degradation rate for both of individual and mixed compounds solution for TiO_2/Sn2, 2.0099 and 1.5441 h^{-1} respectively. Phenol solution presented the highest degradation rate, 0.5446 h^{-1}, for individual solution with commercial TiO_2. Mixed compounds solution, phenol showed the lowest degradation rate, 0.0392 and 0.0406 h^{-1}, for photocatalysts TiO_2/Sn2 and commercial TiO_2 respectively.

Table 4-7 Photocatalysis reaction rate of phenolic compounds

Phenolic compounds	k_{obs} (h^{-1})	R^2
Individual compounds		
TiO_2/Sn2		
• Phenol	0.1529	0.9581
• Guaiacol	0.4973	0.9611
• Syringol	2.0099	0.9272
Commercial TiO_2		
• Phenol	0.5446	0.9109
• Guaiacol	0.3863	0.9161
• Syringol	0.2057	0.9636
Mixed compounds		
TiO_2/Sn2		
• Phenol	0.0392	0.9581
• Guaiacol	0.3133	0.9467
• Syringol	1.5441	0.9147
Commercial TiO_2		
• Phenol	0.0406	0.9352
• Guaiacol	0.1336	0.9661
• Syringol	0.1776	0.9792

In summary, photocatalytic degradation of the individual and mixed phenolic compounds by the synthesized TiO_2/Sn2 and the commercial TiO_2 were significantly different. The TiO_2/Sn2 presented the consistency of photocatalytic degradation of both individual and mixed phenolic compound solution. It also presented the highest degradation efficiency of methoxy phenol while the commercial TiO_2 presented the inconsistency of the degradation between the mixed and individual compounds. The commercial one presented the higher degradation for the individual solution of phenol. The phenol degradation efficiency was substantially decreased for the mixed solution. Furthermore, the phase components of the catalysts, combination of anatase and rutile of the synthesized one or only anatase phase of the commercial one influenced on intermediates generation which then further to the photocatalytic degradation.

In addition, as the wastewater contain the mixed phenolic compounds, the synthesized one yielded rather higher degradation of phenolic compounds than the commercial one. Therefore, the synthesized TiO_2/Sn2 has a potential to use as catalyst on degradation of phenolic contaminated wastewater. Moreover, further study (such as irradiation time, intermediates) for degradation of the mixed solution particularly for phenol is required.

4.5 Photocatalytic Reaction: Pulp and Paper Wastewater

Real wastewater was taken from the pulp and paper mill (pH=11.74) for studying the photocatalytic potential of commercial TiO_2 and TiO_2/Sn2. The initial concentration of the real wastewater was measured by GC/FID technique. The contents were 0.0235, 0.3613 and 0.2097 mg/l for phenol, guaiacol and syringol respectively. After 6 hours irradiation, the degradation for phenol, guaiacol and syringol 51% , 51%, and 58% , respectively for the commercial TiO_2. The degradation efficiency of phenol, guaiacol and syringol 87% , 25%, and 37%, respectively for TiO_2/Sn2.

Pattern of the photodegradation of phenolic compounds of the real wastewater was demonstrated by the plot of concentration of phenolic compounds along the irridiation time as shown in Figure 4-16. The graphical line of phenol degradation represented a very small change of concentration along the time for both photocatalysts. Dramatically, guaiacol and syringol were changed for both synthesized TiO_2/Sn2 and commercial TiO_2. However, the degradation rate by the commercial TiO_2 significantly changed for the first 4 hours, and then it was almost constantly slow. The synthesized TiO_2/Sn2 expressed a significant change along the time up to 6 hours of experimental time. It was likely stated that the synthesized TiO_2/Sn2 exhibited the better performance for the mixed phenolic compounds in real wastewater. This performance was the same as the results obtained from the synthetic mixed phenolic compound solution. However, as mentioned previously both commercial and synthesized ones could not perform well on phenol degradation in the mixed phenolic compound solution. This is possibly due to the irradiation time was not long enough.

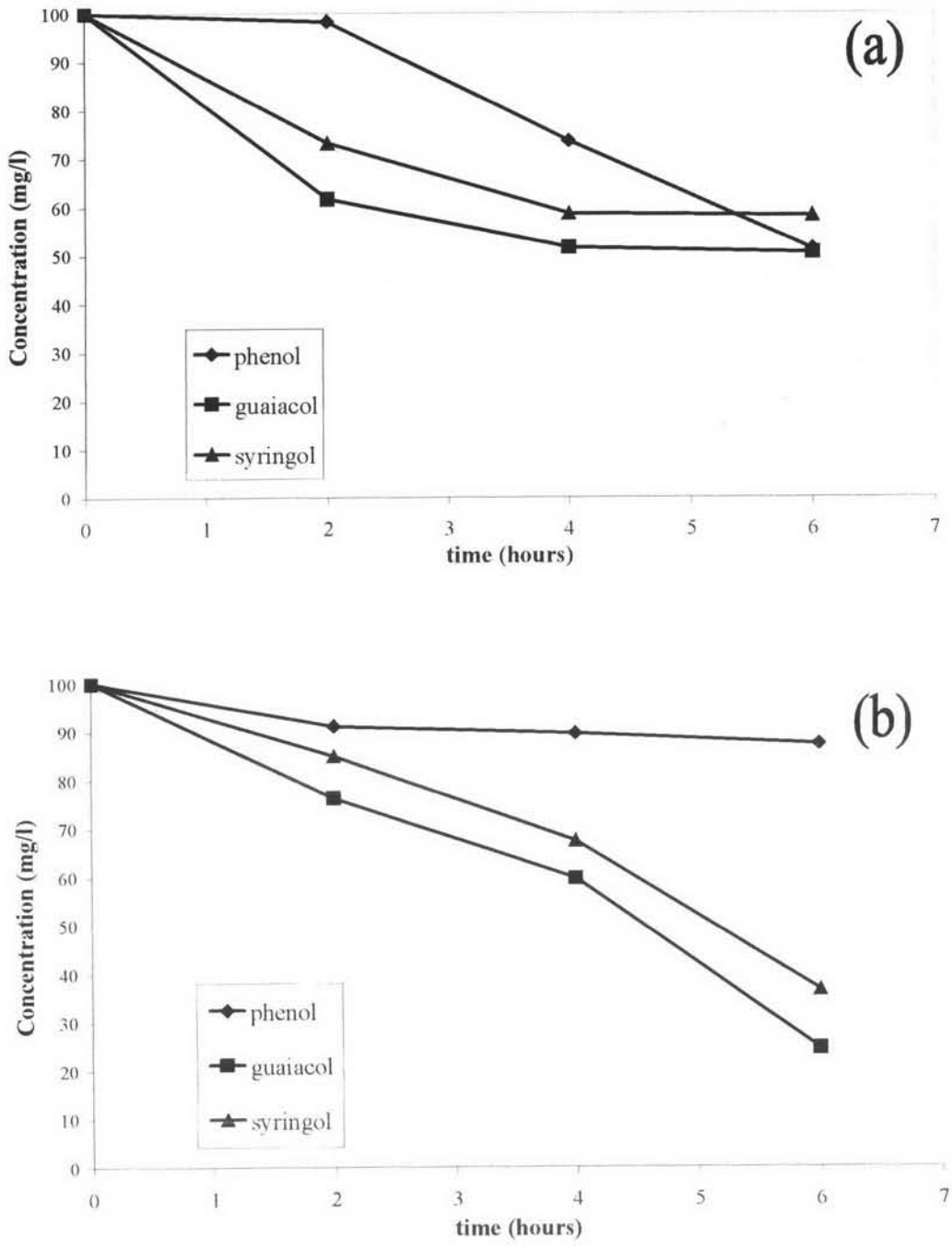

Figure 4-16 Photocatalytic degradation of pulp and paper wastewater (a) Commercial TiO_2 (b) TiO_2/Sn2.

4.5.1 Summary

Wastewater from pulp and paper mill very complex by many phenolic compounds which contained in wastewater and the color showed a dark brown. These matrixes were the inhibition to the suspended photocatalytic degradation. Thus phenolic compounds slightly show a lower degradation than synthetic wastewater but the TiO_2/Sn2 showed a high potential to degrade the guaiacol and syringol which are high amount of concentration in the pulp and paper mill wastewater. The limitation of the vessel batch reactor may is the constrain to photacatalytic degradation, the well design reactor and also immobilized photocatalysts on the fixed surface and design a low depth of water in reactor may increase the efficiency of phenolic degradation